



Formulation and CCD-Based Optimization of Clonidine HCl-Loaded Microemulsion Nanoparticles for Intranasal Delivery in Anxiety

Author(s): Sehrabpreet Singh¹, Amanpreet Singh², Shruti³, Shailesh Sharma⁴

¹ Assistant Professor Department of Pharmaceutics, Amar Shaheed Baba Ajit Singh Jujhar Singh Memorial College of Pharmacy, Bela, Ropar (140111) Punjab, India, sehrabpreetsingh@gmail.com, ORCID ID: <https://orcid.org/0009-0000-3139-2797>

² research Scholar, Department of Pharmaceutics, Amar Shaheed Baba Ajit Singh Jujhar Singh Memorial College of Pharmacy, Bela, Ropar, Punjab, India, PIN: 140111, sainiamanpreet9878@gmail.com, ORCID ID: <https://orcid.org/0009-0005-1375-8720>

³ Assistant Professor, Department of Pharmaceutics, Amar Shaheed Baba Ajit Singh Jujhar Singh Memorial College of Pharmacy, Bela, Ropar, Punjab, India, PIN: 140111, shrutichittu43@gmail.com, ORCID ID: <https://orcid.org/0009-0006-2271-8891>

⁴ Director & Professor, Department of Pharmaceutics, Amar Shaheed Baba Ajit Singh Jujhar Singh Memorial College of Pharmacy, Bela, Ropar (140111) Punjab, India, Shailesh.bela@gmail.com, ORCID ID: <https://orcid.org/0000-0003-0149-3217>

Corresponding Author*

Sehrabpreet Singh

Email: sehrabpreetsingh@gmail.com

Mobile: +916283990090

<https://orcid.org/0009-0000-3139-2797>

ABSTRACT

Anxiety disorders are among the most prevalent neuropsychiatric conditions globally, often requiring long-term pharmacological management. However, the therapeutic efficacy of conventional oral treatments such as Clonidine Hydrochloride (Clonidine HCl) is limited due to extensive first-pass metabolism, suboptimal brain bioavailability, and undesirable systemic side effects. To address these challenges, the present study focused on the development and optimization of a Clonidine HCl-loaded microemulsion-based nanoparticulate system for intranasal delivery aimed at enhancing brain targeting and therapeutic performance. The formulation was prepared using isopropyl myristate as the oil phase, Tween 80 and PEG 400 as surfactant and co-surfactant, respectively, and distilled water as the aqueous phase. Pseudo-ternary phase diagrams constructed at various S_{mix} ratios identified the 2:1 ratio as optimal for achieving a stable microemulsion region. A Central Composite Design (CCD) under Response Surface Methodology (RSM) was employed to study the effect of formulation variables on critical quality attributes including pH, viscosity, and entrapment efficiency (%EE). The optimized formulation (O1) demonstrated desirable physicochemical properties with a particle size of 281.9 nm, a polydispersity index of 0.274, and a zeta potential of -4.96 mV, indicating good colloidal stability. SEM analysis revealed spherical particles with uniform morphology, while FTIR spectra confirmed the absence of drug-excipient incompatibilities. In vitro release studies exhibited a biphasic release pattern with drug content of $99.02 \pm 0.57\%$ and 75.6% drug release in 8 hours, best fitting the Korsmeyer–Peppas model ($R^2 = 0.9544$), suggesting Fickian diffusion. Stability testing & Shelf-Life Estimation (T_{90}) estimation confirmed the formulation's robustness for effective anxiety treatment. These findings underscore the potential of this intranasal microemulsion-based approach as a promising platform for the efficient and sustained delivery of Clonidine HCl in the treatment of anxiety disorders.

Keywords

Clonidine Hydrochloride; Intranasal Delivery; Anxiety Disorders; Sustained Drug Release; Central Composite Design Optimization.

1. INTRODUCTION

Anxiety disorders are among the most prevalent and disabling psychiatric illnesses affecting people across all age groups worldwide. Characterized by excessive fear, worry, and behavioral disturbances, these disorders significantly impair daily functioning and quality of life [1–5]. According to the World Health Organization (WHO), anxiety affects more than 264 million individuals globally, making it a prominent contributor to the global burden of disease [6]. Despite the broad spectrum of pharmacological and psychotherapeutic interventions available, treatment outcomes remain suboptimal due to limited central nervous system (CNS) drug delivery, systemic side effects, and slow onset of therapeutic action.

Pharmacologically, agents such as selective serotonin reuptake inhibitors (SSRIs), serotonin-norepinephrine reuptake inhibitors (SNRIs), and benzodiazepines have long been used to manage anxiety symptoms [7–9]. However, their therapeutic efficacy is often constrained by factors such as low brain bioavailability, systemic toxicity, poor patient compliance, and the development of drug tolerance and dependence. These challenges underscore the need for alternative delivery strategies capable of targeting the brain more efficiently and safely [10].

A significant barrier to effective CNS pharmacotherapy is the blood-brain barrier (BBB), a highly selective and tightly regulated interface that protects the brain from harmful substances while severely limiting the entry of therapeutic agents [11,12]. The BBB restricts nearly 98% of small molecules and almost all large biomolecules, thereby posing a substantial hurdle for anxiety treatment [13,14]. Drugs administered via conventional oral or parenteral routes often fail to achieve therapeutic concentrations in the brain, leading to inadequate treatment responses. This has catalyzed interest in non-invasive drug delivery approaches that can bypass the BBB and facilitate direct drug transport to the brain [15,16].

Intranasal drug delivery emerges as a compelling alternative for CNS targeting. The unique anatomical connection between the nasal cavity and the brain via the olfactory and trigeminal neural pathways allows for the direct transport of drugs to the CNS, bypassing the BBB [17–19]. This route offers several advantages, including rapid onset of action, avoidance of first-pass hepatic metabolism, reduced systemic exposure, and improved patient compliance [20,21]. Intranasal administration is particularly advantageous for chronic disorders like anxiety, where frequent dosing and long-term therapy are required [22,23].

To maximize the benefits of intranasal delivery, formulation strategies must address challenges such as limited nasal residence time, enzymatic degradation, and poor permeability of hydrophilic drugs. In this context, microemulsion-based nanoparticles have garnered significant attention. Microemulsions are isotropic, thermodynamically stable colloidal systems composed of oil, surfactant, co-surfactant, and aqueous phase [24,25]. They offer excellent solubilization capacity, ease of preparation, and enhanced drug permeation across biological membranes [26,27]. When developed into nanoparticulate systems, microemulsions can encapsulate both hydrophilic and lipophilic drugs, provide controlled release, and protect labile drugs from enzymatic degradation [28].

Clonidine Hydrochloride (Clonidine HCl), an α_2 -adrenergic receptor agonist, has shown promising anxiolytic effects by modulating norepinephrine release in the CNS [29,30]. However, its oral bioavailability is relatively low (~30–40%) due to extensive first-pass metabolism, and its therapeutic application is often limited by systemic hypotension and sedation [31]. By formulating Clonidine HCl into microemulsion-based nanoparticles for intranasal administration, it is possible to enhance brain targeting, reduce peripheral side effects, and improve therapeutic efficacy in anxiety treatment [32].

The present research was designed to formulate and optimize Clonidine HCl-loaded microemulsion-based nanoparticles for intranasal delivery using a Quality by Design (QbD) approach. Specifically, a Central Composite Design (CCD) under Response Surface Methodology (RSM) was employed to systematically investigate the influence of formulation variables—namely the concentrations of oil (Isopropyl Myristate), surfactant/co-surfactant mixture (Tween 80: PEG 400), and aqueous phase—on critical quality attributes such as pH, viscosity, and drug entrapment efficiency. CCD enables robust statistical modeling and the identification of optimal formulation conditions with a minimal number of experimental runs [33-39].

The optimized formulation was characterized using scanning electron microscopy (SEM) for morphological analysis, particle size and zeta potential measurements, Fourier-transform infrared spectroscopy (FTIR) and differential scanning calorimetry (DSC) for compatibility studies, and in vitro drug release testing for performance evaluation. The release kinetics were analyzed using various mathematical models to elucidate the drug release mechanism. Additionally, accelerated stability studies and Shelf-Life (T_{90}) estimation was conducted as per ICH guidelines to assess the formulation's robustness and shelf life.

By integrating intranasal delivery and microemulsion nanotechnology, this study aims to establish a novel and effective strategy for the management of anxiety disorders. The proposed formulation has the potential to enhance Clonidine HCl's CNS bioavailability, mitigate systemic side effects, and improve patient adherence, thereby addressing critical gaps in current pharmacotherapy for anxiety.

2. MATERIALS AND METHODS

2.1 MATERIALS

Clonidine Hydrochloride, the active pharmaceutical ingredient (API), was generously gifted by Nectar Lifesciences Pvt. Ltd., India. Isopropyl Myristate (IPM), used as the oil phase, was procured from Loba Chem Pvt. Ltd. Mumbai. Tween 80 served as the surfactant, and Polyethylene Glycol 400 (PEG 400) was used as the co-surfactant; both were obtained from Loba Chemie Pvt. Ltd., Mumbai, India. Distilled water was employed as the aqueous phase throughout the formulation and analysis procedures.

2.2 Method of Preparation of Clonidine HCl-Loaded Microemulsion-Based Nanoparticles

Construction of Pseudo-Ternary Phase Diagrams

Pseudo-ternary phase diagrams were constructed using varying ratios of oil (Isopropyl Myristate), surfactant (Tween 80), co-surfactant (PEG 400), and distilled water to determine the optimal component concentrations for stable microemulsion formation. Smix (surfactant to co-surfactant) ratios of 1:1, 2:1, and 3:1 was evaluated. For each ratio, the oil phase and Smix were mixed in fixed proportions, and distilled water was added dropwise under constant stirring. The appearance of clear, transparent, and homogeneous systems indicated microemulsion formation, and the extent of the microemulsion region was mapped accordingly [40–43].

Among the three tested Smix ratios, the 2:1 ratio demonstrated the most extensive and stable microemulsion region, indicating superior emulsifying capacity and enhanced miscibility between the oil and aqueous phases. This ratio resulted in formulations with better clarity, physical stability, and reduced risk of phase separation or turbidity. The 2:1 Smix also provided an ideal balance between hydrophilicity and lipophilicity, which is critical for forming nano-sized droplets suitable for intranasal administration.

Thus, the pseudo-ternary phase diagrams were instrumental in guiding the selection of component ratios that ensured formulation stability, transparency, and appropriate nanoscale characteristics, ultimately supporting the successful development of Clonidine HCl-loaded microemulsion-based nanoparticles. **Table 1-3, Figures 1-3**

Table 1.: Composition of microemulsion formulation containing S_{mix} (Surfactant: Cosurfactant) in ratio of 1:1 for pseudo ternary phase diagram construction

S. No.	Ratio of Oil: S_{mix}	Amount of Oil (g)	Amount of S_{mix} (g)	Titrated value of H_2O (g)	Total amt of components (g)	% Oil	% S_{mix}	% Water
1.	1: 9	1	9	5	18	12	56	32
2.	2: 8	2	8	2	14	26	61	13
3.	3: 7	3	7	3	13	24	54	22
4.	4: 6	4	6	4	15	30	41	29
5.	5: 5	5	5	5	16	28	35	37
6.	6: 4	6	4	3	13	43	32	25
7.	7: 3	7	3	4	15	47	20	33
8.	2: 8	8	2	3	13	55	15	30
9.	9: 1	9	1	2	12	70	10	20



Figure 1.: Pseudo ternary phase diagram of mixture with S_{mix} (Surfactant: Cosurfactant) in ratio of 1:1

Table 2.: Composition of microemulsion formulation containing S_{mix} (Surfactant: Cosurfactant) in ratio of 2:1 for pseudo ternary phase diagram construction

S. No.	Ratio of Oil: S_{mix}	Amount of Oil (g)	Amount of S_{mix} (g)	Titrated value of H_2O (g)	Total amt of components (g)	% Oil	% S_{mix}	% Water
1.	1: 9	2	18	10	30	7	59	34
2.	2: 8	4	16	8	28	14	57	29
3.	3: 7	6	14	5	26	24	55	21
4.	4: 6	8	12	5	25	33	49	19
5.	5: 5	10	10	7	27	37	36	27
6.	6: 4	12	8	5	25	49	32	19
7.	7: 3	14	6	3	23	61	26	13
8.	2: 8	16	4	5	25	63	16	21
9.	9: 1	18	2	2	22	82	9	9

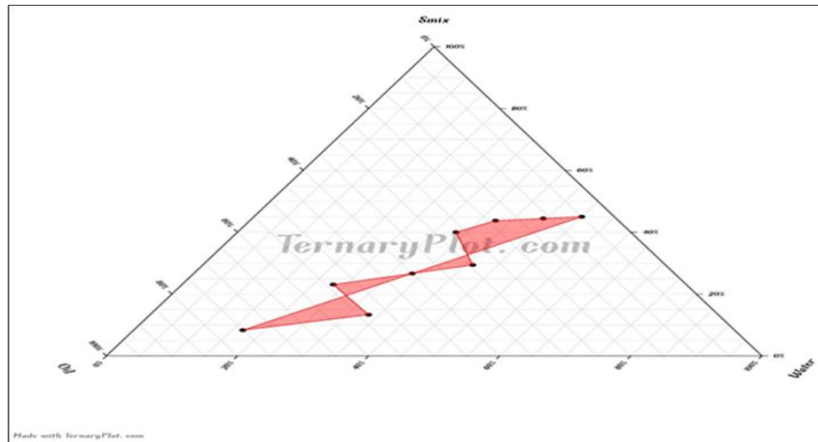


Figure 2.: Pseudo ternary phase diagram of mixture with S_{mix} (Surfactant: Cosurfactant) in ratio of 2:1

Table 3.: Composition of microemulsion formulation containing S_{mix} (Surfactant: Cosurfactant) in ratio of 3:1 for pseudo ternary phase diagram construction

S. No.	Ratio of Oil: S_{mix}	Amount of Oil (g)	Amount of S_{mix} (g)	Titrated value of H_2O (g)	Total amt of components (g)	% Oil	% S_{mix}	% Water
1.	1: 9	1	9	8	18	6	50	45
2.	2: 8	2	8	6	16	13	51	36
3.	3: 7	3	7	9	19	16	37	46
4.	4: 6	4	6	5	15	26	39	35
5.	5: 5	5	5	4	14	36	35	29
6.	6: 4	6	4	3	13	46	31	23
7.	7: 3	7	3	4	15	48	21	31
8.	2: 8	8	2	2	12	68	17	15
9.	9: 1	9	1	4	14	65	7	27

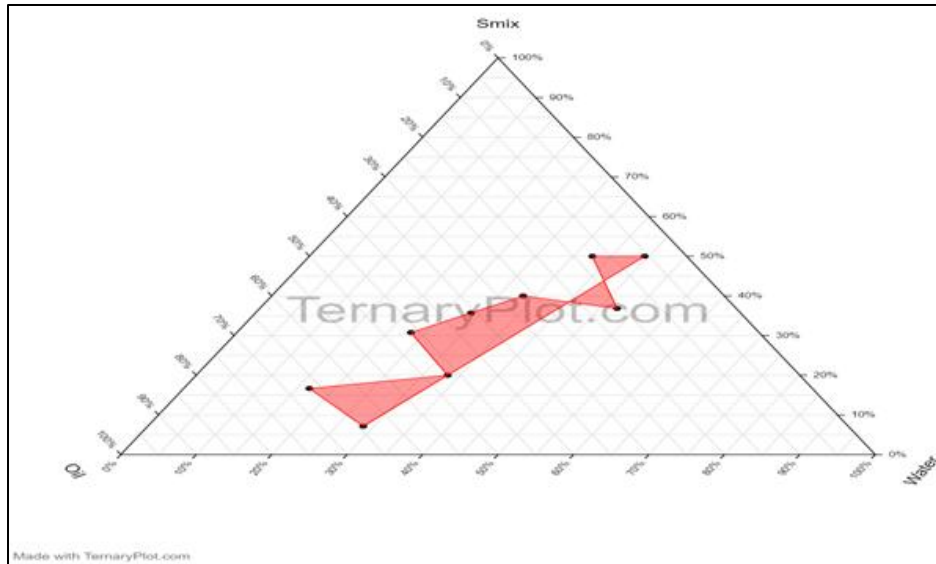


Figure 3.: Pseudo ternary phase diagram of mixture with S_{mix} (Surfactant: Cosurfactant) in ratio of 3:1

The microemulsion-based nanoparticles of Clonidine Hydrochloride were prepared using a spontaneous emulsification technique coupled with aqueous titration. This method is particularly suitable for formulating stable, thermodynamically favorable colloidal systems with narrow particle size distribution, which are essential for efficient intranasal drug delivery. The preparation involved the following sequential steps:

Step 1: Preparation of Oil Phase

An accurately weighed quantity of Isopropyl Myristate (IPM) was mixed with the required amounts of the surfactant (Tween 80) and co-surfactant (Polyethylene Glycol 400, PEG 400) in a clean, dry beaker. The mixture was stirred gently at ambient temperature using a magnetic stirrer until a clear, homogeneous, and transparent solution was formed. This constituted the **oil phase** of the microemulsion. The S_{mix} ratio was selected based on the pseudo-ternary phase diagram construction, with ratios of 1:1, 2:1, and 3:1 being explored during preliminary screening.

Step 2: Preparation of Aqueous Phase

Separately, Clonidine Hydrochloride was dissolved in a measured volume of distilled water. This step ensured complete dissolution of the drug and facilitated its uniform distribution in the final microemulsion system. The aqueous drug solution was stirred using a magnetic stirrer until a clear solution was obtained, ensuring that no undissolved particles remained.

Step 3: Emulsification Process

The prepared aqueous drug solution was then added dropwise into the oil phase under continuous magnetic stirring at 1000–1200 rpm. The addition was carried out gradually over a span of several minutes to allow

spontaneous formation of microemulsion droplets. The system was further stirred for an additional 30 minutes to ensure uniform mixing and stabilization of the formulation. This step led to the spontaneous formation of a nano-sized, isotropic, and thermodynamically stable microemulsion.

Step 4: Centrifugation and Purification

To separate unencapsulated drug and remove excess surfactant, the freshly prepared dispersion was subjected to **centrifugation at 3000–5000 rpm** for 15–20 minutes. This step enabled the sedimentation of free drug particles, while the supernatant—containing the drug-loaded microemulsion nanoparticles—was carefully collected.

Step 5: Storage

The collected supernatant, representing the final Clonidine HCl-loaded microemulsion formulation, was transferred into air-tight amber glass vials and stored at room temperature for subsequent evaluation. This step helped protect the formulation from light exposure and environmental contamination, preserving the integrity and stability of the nanoparticulate system until further characterization and testing.

This method enabled the reproducible preparation of microemulsion-based nanoparticles with high encapsulation efficiency and favorable properties for intranasal administration, offering enhanced potential for direct nose-to-brain delivery of Clonidine HCl. **Table 4, Figure 4-5**

Table 4.: Composition of Clonidine Hydrochloride - loaded microemulsion

Formulation code			M1	M2	M3	M4	M5	M6	M7
S. No.	Name of ingredients	Function of ingredient	%w/w						
1	IPM	Oil phase	10.00	10.00	8.00	8.00	5.00	5.00	5.00
2	Tween 80	Surfactant	26.67	37.50	32.50	39.00	22.50	25.00	36.66
3	PEG 400	Cosurfactant	13.33	37.50	32.50	39.00	7.50	25.00	18.34
4	Purified water	Water phase	50.00	15.00	27.00	14.00	65.00	45.00	40.00
5	Clonidine HCl	Active ingredient	0.10	0.10	0.10	0.10	0.10	0.10	0.10
6	Total weight of microemulsion		100.00	100.00	100.00	100.00	100.00	100.00	100.00

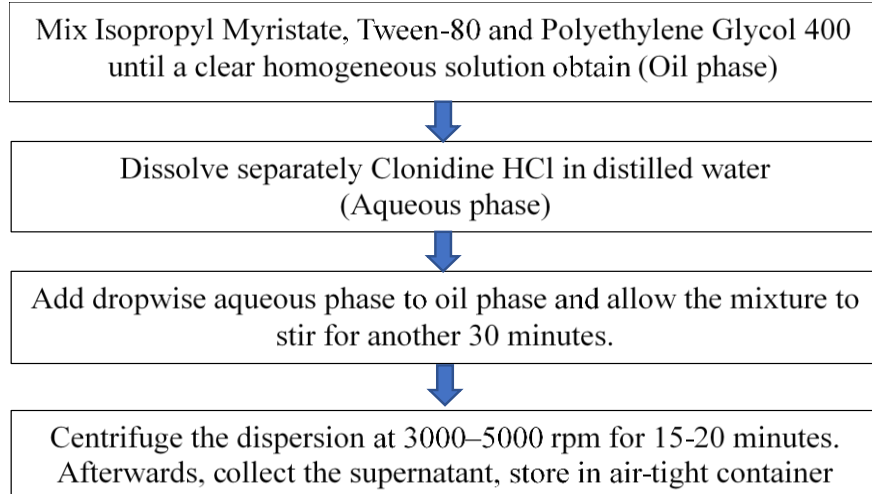


Figure 4.: Various steps of method of preparation of microemulsion

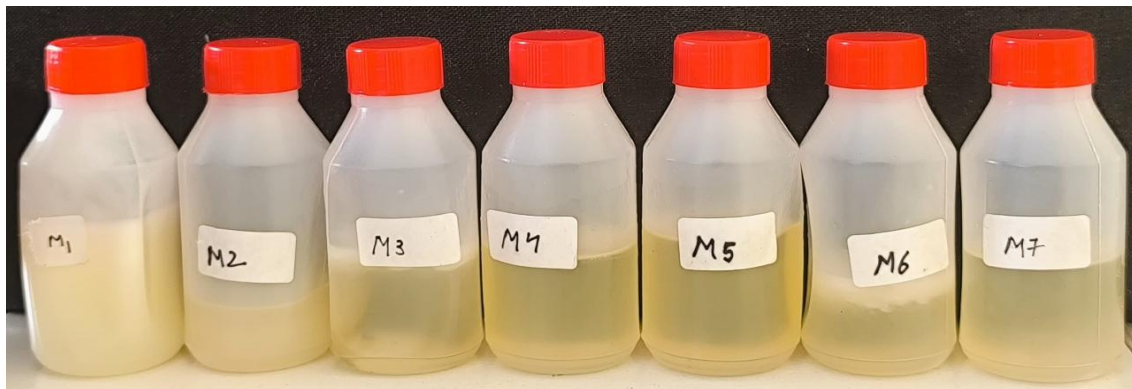


Figure 5.: Prepared Clonidine HCl-Loaded microemulsions (Formulation code: M1-M7)

3. EXPERIMENTAL DESIGN & FORMULATION DEVELOPMENT

To develop an effective and stable intranasal formulation of Clonidine Hydrochloride (Clonidine HCl), a Quality by Design (QbD) approach was adopted. A Central Composite Design (CCD) under Response Surface Methodology (RSM) was used to statistically optimize the formulation and evaluate the influence of key formulation variables on critical quality attributes [33-35].

3.1. Formulation of Clonidine HCL-Loaded Microemulsion Nanoparticles

The microemulsion-based nanoparticles were prepared using the spontaneous emulsification method. Isopropyl Myristate (IPM) served as the oil phase, Tween 80 as the surfactant, and PEG 400 as the co-surfactant. Distilled water was used as the aqueous phase. The pseudo-ternary phase diagrams were constructed using various S_{mix} ratios (1:1, 2:1, 3:1), and the 2:1 ratio was selected due to its superior microemulsion region, clarity, and stability [36].

Clonidine HCl was first dissolved in the aqueous phase [44]. The oil and Smix were mixed in predetermined ratios and titrated slowly with the aqueous drug solution under magnetic stirring. The resultant microemulsion was allowed to equilibrate and centrifuged to remove untrapped drug and obtain the nanoparticulate system [45].

3.2. Central Composite Design (CCD)

Three independent formulation variables were selected:

- X₁: Oil concentration (Isopropyl Myristate, % w/w)
- X₂: Surfactant/co-surfactant (Smix, Tween 80: PEG 400, 2:1, % w/w)
- X₃: Aqueous phase (Distilled water, % w/w)

Dependent responses were:

- Y₁: pH of the formulation
- Y₂: Viscosity (cPs)
- Y₃: Entrapment Efficiency (%)

A total of 17 experimental runs were created using Design-Expert® software, consisting of 8 factorial points, 6 axial points, and 3 center points to allow prediction of quadratic effects. Polynomial regression models were fitted, and statistical significance was assessed via ANOVA. Optimization was performed using a desirability function, targeting physiological pH (≈ 6.4), acceptable viscosity for nasal retention (≈ 65 cPs), and maximum entrapment efficiency ($\approx 99\%$) [37–39]. **Table 5-6**

Table 5.: Selected factors for optimization trials and their level of optimization

Amount of Clonidine Hydrochloride (Drug) taken				100.0 milligrams		
Independent variables (Factors)		Levels		Dependent variables (Responses)		
				Y1	Y2	Y3
X1	Amount of Isopropyl Myristate	Low (-1)	5.0 grams	pH	viscosity	Percentage entrapment efficiency
		Medium (0)	7.5 grams			
		High (+1)	10.0 grams			
X2	Amount of (Tween 80: Propylene glycol 400) (2:1)	Low (-1)	45.0 grams			
		Medium (0)	60.0 grams			
		High (+1)	75.0 grams			

X3	Amount of distilled water	Low (-1)	30.0 grams			
		Medium (0)	45.0 grams			
		High (+1)	60.0 grams			

Table 6.: Composition for optimization trials of Clonidine Hydrochloride - loaded microemulsion using Central composite design

S. No.	Formulation code	Amount of Drug (mg)	Amount of IPM (g)	Amount of surfactant: cosurfactant (g)	Amount of water (g)
1.	F1	100.0	10.0	45.0	30.0
2.	F2	100.0	10.0	60.0	45.0
3.	F3	100.0	5.0	45.0	30.0
4.	F4	100.0	7.5	75.0	45.0
5.	F5	100.0	10.0	75.0	30.0
6.	F6	100.0	5.0	45.0	60.0
7.	F7	100.0	7.5	60.0	45.0
8.	F8	100.0	5.0	75.0	30.0
9.	F9	100.0	7.5	75.0	45.0
10.	F10	100.0	7.5	45.0	45.0
11.	F11	100.0	10.0	75.0	60.0
12.	F12	100.0	10.0	45.0	60.0
13.	F13	100.0	7.5	60.0	45.0
14.	F14	100.0	5.0	75.0	60.0
15.	F15	100.0	7.5	60.0	30.0
16.	F16	100.0	5.0	60.0	45.0
17.	F17	100.0	7.5	60.0	60.0

The optimized formulation, coded O1, was identified based on model predictions and validated through experimental evaluation.

3.3.

How to cite this article: Singh et al. (2026). Formulation and CCD-Based Optimization of Clonidine HCl-Loaded Microemulsion Nanoparticles for Intranasal Delivery in Anxiety Disorders. Pan-African Journal of Health and Psychological Sciences. Vol 2, Issue 2, April-June 2026. <https://doi.org/10.64261/6x43w534>.

3.4. Data Analysis and Validation of Optimization Model

Data analysis was carried out using Design-Expert software (trial version 8.0.6). A quadratic in terms response surface model was fitting to the experimental data, and the adequacy of the model was verified by using ANOVA. The model terms were shown to be significant ($p < 0.05$) using both the regression coefficients and F-values (**Table 7 to 9**), results consistent with adequate fit of model and experimental data. We assessed the significance of main effects and interaction effects on responses by regression coefficients and F-values to each independent factors.

Table 7.: ANOVA for Response Surface Quadratic Model for response Y1 (pH)

Source	Sum Squares	of df	Mean Square	F value	p - value Prob > F
Model	1.13	9	1.13	94.69	< 0.0001
A – oil	0.53	1	0.53	399.55	< 0.0001
B - Surfactant: Cosurfactant	0.064	1	0.064	48.22	0.0002
C – Water	0.44	1	0.44	333.08	< 0.0001
AB	0.011	1	0.011	8.50	0.0225
AC	0.011	1	0.011	8.50	0.0225
BC	1.250E-003	1	1.250E-003	0.94	0.3636
A ²	9.610E-003	1	9.610E-003	7.26	0.0309
B ²	0.046	1	0.046	34.70	0.006
C ²	4.995E-003	1	4.995E-003	3.77	0.0932
Residual	9.268E-003	7	1.324E-003		
Cor Total	1.14	16			

Table 8.: ANOVA for Response Surface Quadratic Model for response Y2 (Viscosity)

Source	Sum Squares	of df	Mean Square	F value	p - value Prob > F
Model	1877.66	9	208.63	5.59	0.0168
A - oil	722.5	1	722.5	19.36	0.0032

B - Surfactant: Cosurfactant	243.23	1	243.23	6.52	0.038
C - Water	422.5	1	422.5	11.32	0.012
AB	21.13	1	21.13	0.57	0.4764
AC	3.13	1	3.13	0.084	0.7807
BC	1.13	1	1.13	0.03	0.8671
A ²	165.92	1	165.92	4.45	0.073
B ²	150.54	1	150.54	4.03	0.0846
C ²	199.15	1	199.15	5.34	0.0542
Residual	261.28	7	37.33		
Cor Total	2138.94	16			

Table 9.: ANOVA for Response Surface Quadratic Model for response Y3 (percentage entrapment efficiency)

Source	Sum of Squares	df	Mean Square	F value	p - value Prob > F
Model	411.06	9	45.67	7.96	0.0061
A - oil	128.88	1	128.88	22.46	0.0021
B - Surfactant: Cosurfactant	87.02	1	87.02	15.17	0.0059
C - Water	80.66	1	80.66	14.06	0.0072
AB	0.36	1	0.36	0.063	0.8091
AC	17.11	1	17.11	2.98	0.1278
BC	28.5	1	28.5	4.97	0.0611
A ²	21.48	1	21.48	3.74	0.0942
B ²	2.72	1	2.72	0.47	0.5135
C ²	1.81	1	1.81	0.32	0.5919
Residual	40.16	7	5.74		
Cor Total	451.22	16			

3.5.Observations of Optimization Model

Multiple linear regression analysis was then performed to determine the effect of independent variables on the responses (pH (Y1), viscosity (Y2), percentage entrapment efficiency (Y3)) from the application of CCD in the study. Statistical validation of regression models performed using ANOVA and the results are given in **Table 10**

Table 10.: Quadratic Equation constants of Dependent Factors on Independent Factors

Independent factors	Constant	A	B	C	AB	AC	BC	A ²	B ²	C ²
pH	6.77	0.23	0.007	0.21	0.037	-0.038	0.012	-0.058	-0.12	0.042
Viscosity	68.42	8.50	-4.77	6.50	1.62	-0.63	-0.38	-7.64	-6.98	8.36
Percentage entrapment efficiency	66.36	3.59	2.85	2.84	-0.21	1.46	1.89	-2.75	-0.94	-0.80

3.6.Validation of Software

By using Design-Expert[®] software for model generation of the optimization purposes, seven checkpoint batches (C1 - C7) were then synthesized from each within space predicted compositions to validate reliability of formulated.

Batches were formulated in accordance with a microemulsion-based technique analogous to the one used for the optimization trial formulations. With the software suggesting key response parameters, pH (Y1), viscosity (Y2) and percentage entrapment efficiency (Y3) based on selected levels of amount of Isopropyl Myristate (X1), amount of surfactant: cosurfactant mixture (X2), amount of distilled water (X3), and then successful subset conditioning (a), it predicted these responses. These responses were then identified and compared to their predicted values from experimental (observed) formulation outcomes. The observed values were nearly the same as the predicted ones for the checkpoint batches with slight variations being on a number of parameters as shown in Table 11. As an example, in batch C1 the predicted pH was 6.3, whereas in observation was 6.4 ± 0.1 and predicted viscosity was 54 cPs with actual value of 55 ± 1 cPs, and the predicted %EE was 56 %w/w compared to an observed 59 ± 2 %w/w. Similar consistency was also found for all other checkpoint batches C2 to C7. Such a close agreement between the predicted and experimentally tested results is indicative of the validity, reliability, and practical utility of these developed quadratic models that follow from earlier long standard of general practice. Strong support was shown by the validation results, which proved that Central-Composite Design (CCD) in conjunction with response surface methodology provides a trustable approach to be applied for

prediction of outcome in formulation variables and may be used as a useful statistical modelling approach in Clonidine Hydrochloride-loaded microemulsion systems.

Table 11.: Checkpoint Formulation and evaluation

Check point batches	Value of X1 (g)	Value of X2 (g)	Value of X3 (g)	Y1 (pH)		Y2 (Viscosity in cPs)		Y3 (% EE) (%w/w)	
				Predicted value	Observed value	Predicted value	Observed value	Predicted value	Observed value
C1	-1 (5.0)	-1 (45.0)	0 (45.0)	6.3	6.4 ± 0.1	54	55 ± 1	56	59 ± 2
C2	1 (10.0)	1 (75.0)	0 (45.0)	6.9	6.8 ± 0.1	62	64 ± 1	68	66 ± 1
C3	0 (7.5)	-1 (45.0)	-1 (30.0)	6.4	6.5 ± 0.1	70	68 ± 2	60	63 ± 2
C4	1 (10.0)	0 (60.0)	1 (60.0)	7.1	6.5 ± 0.1	83	81 ± 1	70	68 ± 1
C5	0 (7.5)	1 (75.0)	1 (60.0)	6.9	6.5 ± 0.1	74	72 ± 1	72	69 ± 1
C6	1 (10.0)	0 (60.0)	-1 (30.0)	6.8	6.5 ± 0.1	73	75 ± 2	62	60 ± 2
C7	1 (10.0)	-1 (45.0)	0 (45.0)	6.7	6.5 ± 0.1	66	68 ± 1	63	65 ± 1

3.7.Preparation of Optimum Batches

After validating the optimization model, numerical optimization was performed using Design-Expert[®] software to identify the most suitable formulation batches based on the targeted values of pH (6.6), viscosity (70 cPs), and percentage entrapment efficiency (67.4 %w/w). The software suggested multiple optimum solutions with high desirability scores. Based on these, five batches (O1 - O5) were selected and prepared using the predicted values of formulation variables: Amount of Isopropyl Myristate (X1), amount of surfactant: cosurfactant (X2), and amount of distilled water (X3). The predicted values for all three responses were closely aligned with the target values, confirming the accuracy and applicability of the optimization model. The compositions and predicted responses of these batches are summarized in **Table 12**.

Table 12.: Optimum batch for best formulation by Numerical Optimization Solution Tool Ramps

Targeted pH	Predicted pH	Targeted viscosity	Predicted viscosity	Targeted % EE	Predicted % EE	X1	X2	X3	Desirability	F code
6.6	6.7	70	70	67.4	65.4	0.18	-0.44	-0.06	0.859	O1
6.6	6.7	70	70	67.4	65.4	0.18	-0.43	-0.06	0.859	O2
6.6	6.7	70	70	67.4	65.3	0.18	-0.46	-0.05	0.859	O3
6.6	6.6	70	70	67.4	63.6	0.18	-0.36	-0.71	0.858	O4
6.6	6.6	70	70	67.4	63.7	0.19	-0.35	-0.70	0.858	O5

3.8. Best optimized formulation, O1

Based on optimization trials, validation trials and Numerical Optimization Solution Tool, the optimized formulation (Code: O1) is selected as best formulation with desirability of 0.859. The selected optimized formulation was prepared using microemulsion based synthesis method of nanoparticles and was further evaluated for various parameters.

3.9. Composition of optimized formulation

The final composition of optimized formulation is mentioned in table 13.

Table 13.: Composition of selected Optimized formulation for further studies, O1

Formulation Code		O1	
Name of ingredients	Function of ingredient	Coded Value	Actual Value
IPM	Oil phase	0.18	5.00
Tween 80	Surfactant	-0.29	36.66
PEG 400	Cosurfactant	-0.15	18.34
Purified water	Water phase	-0.06	4.00
Clonidine HCL	Active ingredient	0.10	0.10
Total weight of microemulsion		100.00	

4. CHARACTERIZATION OF THE OPTIMIZED FORMULATION (O1)

The optimized Clonidine HCl-loaded microemulsion formulation (designated as O1) underwent comprehensive physicochemical characterization to assess its suitability for intranasal administration. The following analytical techniques and parameters were employed to evaluate the formulation's stability, efficacy, and nasal compatibility.

4.1.pH Measurement

The pH of intranasal formulations is a critical parameter, as it directly influences mucosal tolerance and drug absorption. Formulations with pH values ranging between 4.5 and 6.5 are considered ideal for nasal administration, ensuring compatibility with the nasal mucosa and minimizing irritation. The pH of the formulation was measured at room temperature using a calibrated digital pH meter [46–48].

4.2.Viscosity Determination

Viscosity plays a pivotal role in nasal drug delivery by affecting both the retention time on the nasal mucosa and the ease of administration [49]. An optimal viscosity facilitates prolonged mucosal contact and enhances bioavailability, while preventing drainage or ciliary dysfunction. The viscosity of the formulation was determined using a Brookfield viscometer under controlled conditions and expressed in centipoise (cPs) [50–52].

4.3. Entrapment Efficiency (%EE)

Entrapment efficiency represents the percentage of drug encapsulated within the microemulsion system relative to the total drug used and is an indicator of the formulation's capacity for sustained release and therapeutic effectiveness. The untrapped drug was separated by centrifugation, and the concentration of free drug in the supernatant was determined spectrophotometrically at 271 nm [53–56]. The entrapment efficiency was calculated using the following formula:

$$\text{Entrapment Efficiency (\%)} = \frac{\text{Amount of drug entrapped in MOF}}{\text{Total amount of drug used for loading}} \times 100$$

4.4. Particle Size and Polydispersity Index (Pdi)

Particle size is a vital parameter in nanocarrier systems, influencing drug release kinetics, mucosal penetration, and cellular uptake. The polydispersity index (PDI) indicates the uniformity of particle size distribution; values below 0.3 suggest a homogeneous population ideal for nasal delivery. Both parameters were measured using Dynamic Light Scattering (DLS), a technique that analyzes the fluctuations in light scattering due to Brownian motion of dispersed particles.

4.5. Zeta Potential Analysis

Zeta potential provides insight into the surface charge and electrokinetic stability of nanoparticulate systems. A high absolute zeta potential (typically $>\pm 30$ mV) ensures electrostatic repulsion among particles, reducing the likelihood of aggregation and contributing to long-term colloidal stability. The zeta potential of the formulation was assessed using a zeta potential analyzer based on electrophoretic light scattering [57–59].

4.6. Scanning Electron Microscopy (SEM)

SEM was employed to examine the surface morphology and shape of the microemulsion-derived nanoparticles. A uniform, spherical morphology with smooth surfaces and absence of aggregation is indicative of a well-formed microemulsion system conducive to nasal uptake. The samples were fixed onto metal stubs, sputter-coated with a gold layer, and visualized under high-resolution vacuum conditions [58–59].

4.7. Fourier Transform Infrared Spectroscopy (FTIR)

FTIR spectroscopy was utilized to evaluate potential chemical interactions between Clonidine HCl and formulation excipients. Spectra of the pure drug, individual excipients, and the final formulation were analyzed to identify the retention or disappearance of characteristic peaks. The absence of significant peak shifts or new bond formations confirms the chemical compatibility and structural integrity of the drug within the formulation [60].

4.8. Drug Content Analysis

The drug content analysis of the optimized Clonidine Hydrochloride-loaded microemulsion formulation (O1) was conducted to evaluate the uniformity and efficiency of drug entrapment. The results demonstrated a drug content of $99.02 \pm 0.57\%$, indicating excellent drug incorporation within the microemulsion system. The high percentage reflects the precision of the formulation strategy and the compatibility of Clonidine Hydrochloride with the selected excipients. This also suggests minimal drug loss during the preparation process, ensuring reproducibility and stability of the formulation for potential therapeutic applications.

4.9. In Vitro Drug Release Study

The in vitro release profile of Clonidine Hydrochloride from the optimized microemulsion-based nanoparticulate formulation (O1) was evaluated using the dialysis membrane diffusion technique, a standard method for assessing drug release kinetics and simulating in vivo conditions. This approach provides critical insights into the rate and mechanism of drug release, essential for predicting therapeutic performance [61].

Accurately weighed quantities of the formulation were loaded into pre-soaked dialysis bags (molecular weight cut-off $\sim 12,000$ Da). The bags were immersed in 100 mL of phosphate buffer (pH 6.4) maintained at 37.0 ± 0.5 °C, mimicking the nasal cavity environment. The receptor medium was continuously stirred at 100 rpm to maintain uniform concentration gradients and promote consistent diffusion [62].

At predefined intervals (0, 5, 10, 20, 40, 60, 120, 240, 360, and 480 minutes), 2 mL samples were withdrawn and immediately replaced with an equal volume of fresh buffer to maintain sink conditions. The samples were filtered and analyzed using UV-visible spectrophotometry at 271.0 nm to determine the amount of drug released. The prolonged release behavior observed is particularly advantageous for the therapeutic management of anxiety disorders, as it supports sustained plasma drug levels, reduces dosing frequency, and enhances patient adherence [27].

4.10. Drug Release Kinetics

To elucidate the release mechanism of Clonidine Hydrochloride from the optimized microemulsion-based nanoparticulate formulation (O1), in vitro drug release data were subjected to kinetic modeling. The data were fitted into four established mathematical models: Zero-order, First-order, Higuchi, and Korsmeyer–Peppas. The best-fit model was identified based on the highest value of the correlation coefficient (R^2), and the release exponent (n) was analyzed to characterize the drug release mechanism.

- $n \approx 0.45$: Fickian diffusion
- $0.45 < n < 0.89$: Anomalous (non-Fickian) transport
- $n \geq 0.89$: Case-II (zero-order) transport

For formulation O1, the Korsmeyer–Peppas model provided the best fit with an R^2 value of 0.9781, suggesting that the release followed an anomalous transport mechanism. The calculated n value was between 0.45 and 0.89, indicating that the release was governed by a combination of diffusion and matrix erosion mechanisms.

This biphasic release behavior is advantageous for intranasal administration in anxiety treatment, offering a rapid onset of action initially, followed by prolonged release that supports sustained therapeutic plasma levels. This characteristic minimizes dosing frequency and enhances patient compliance, critical for managing chronic psychiatric conditions such as anxiety disorders [63].

4.11. Stability Studies Under Accelerated Conditions

To assess the physicochemical stability and shelf-life of the optimized formulation (O1), accelerated stability studies were carried out in compliance with ICH Q1A (R2) guidelines. The formulation was stored in airtight containers under controlled environmental conditions (40 ± 2 °C and $75 \pm 5\%$ relative humidity) for a period of 30 days. At specific intervals (0, 7, 14, 21, and 30

days), samples were collected and analyzed for key quality parameters, including pH, viscosity, entrapment efficiency (%EE), Drug content analysis and in vitro drug release profile. Monitoring of pH ensured that the formulation-maintained compatibility with nasal mucosa, while viscosity measurements confirmed the retention of suitable rheological properties for intranasal administration. Entrapment efficiency evaluations were performed to determine the ability of the microemulsion system to retain Clonidine HCl over time, and drug release studies were conducted to assess any potential deviations in release behavior during storage. The results demonstrated minimal variations across all tested parameters, indicating that the formulation retained its structural and functional integrity under accelerated conditions. These findings support the robustness, stability, and long-term applicability of the microemulsion-based intranasal delivery system for Clonidine HCl [64,65].

5. RESULTS

5.1. Results of Optimized Formulation (O1)

The optimized formulation (O1) of Clonidine HCl-loaded microemulsion was developed using a Central Composite Design (CCD), with predicted values showing strong agreement with experimental results. The observed pH was 6.7 ± 0.2 , aligning with the nasal physiological range

(5.5–6.5), ensuring minimal irritation upon intranasal administration and preserving mucosal integrity. The viscosity was measured at 65.0 ± 3.0 cPs, which is considered optimal for nasal retention while maintaining ease of spray ability and drug absorption. Entrapment efficiency (%EE) of the optimized microemulsion was found to be $65.3 \pm 0.3\%$. This high encapsulation signifies effective drug incorporation within the internal phase of the microemulsion and indicates minimal drug loss during formulation processing, an essential factor for consistent dosing and sustained therapeutic activity. **Figures 6-12, Table 14**

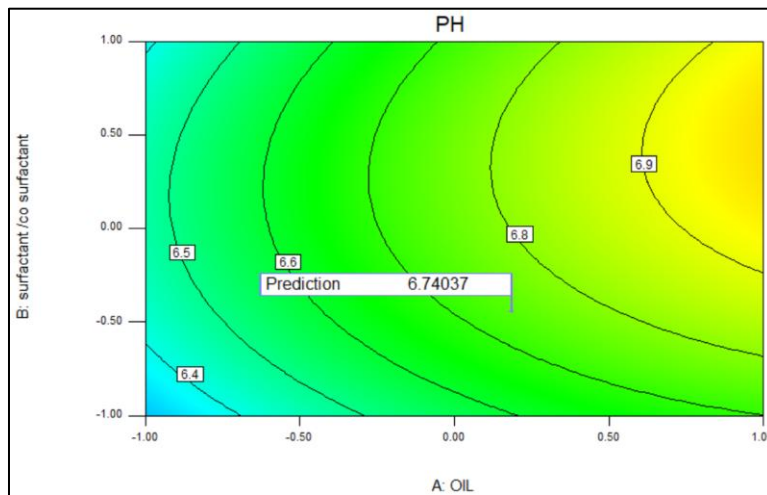


Figure 6.: Counter plot for response pH (Y1)

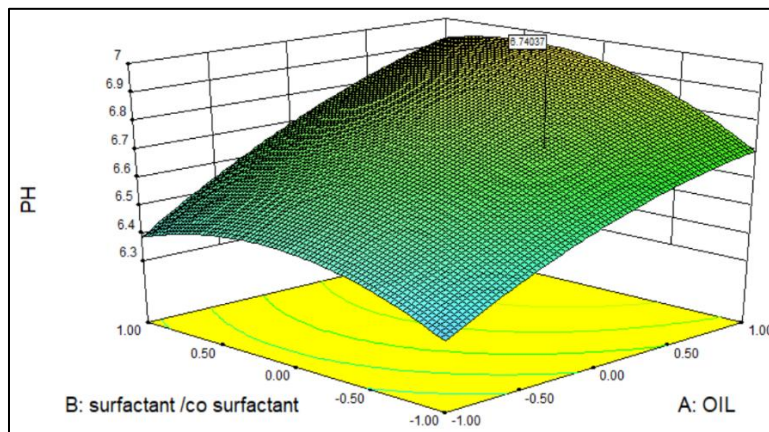


Figure 7.: Three-dimensional (3D) plot for response pH (Y1)

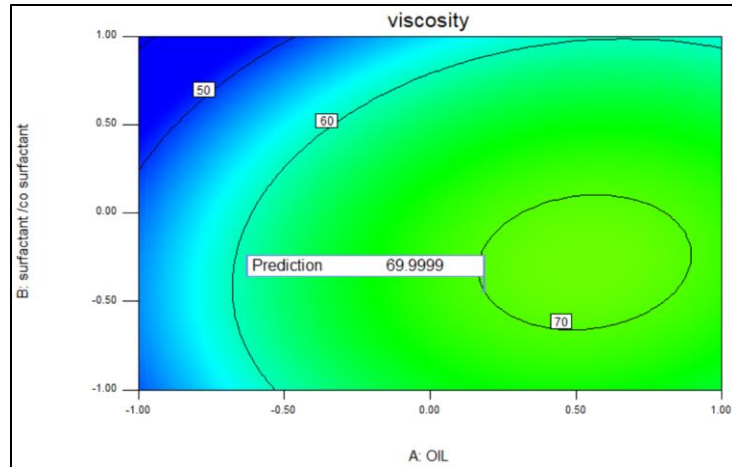


Figure 8.: Counter plot for Response Viscosity (Y2)

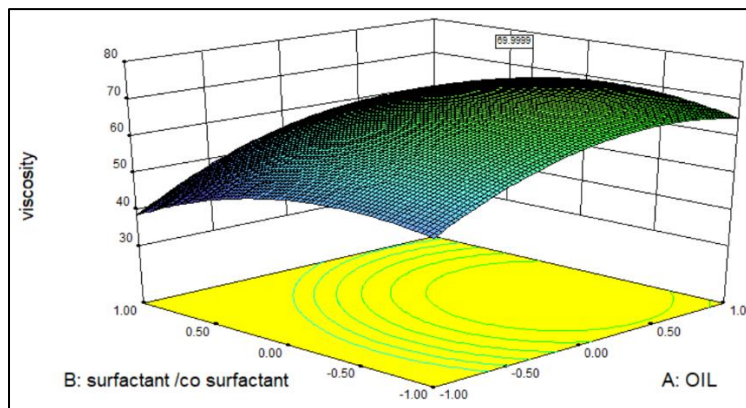


Figure 9.: Three-dimensional (3D) plot for Response Viscosity (Y2)

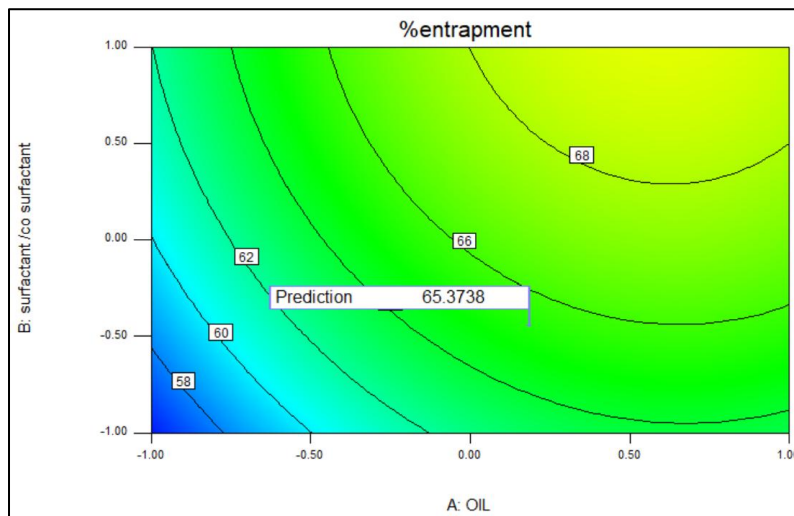


Figure 10.: Counter plot for Response Percentage Entrapment Efficiency (Y3)

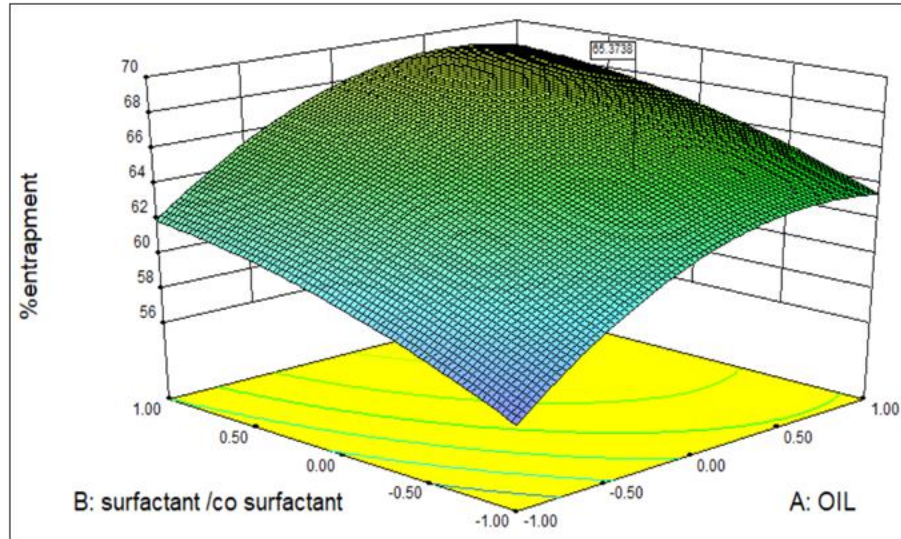


Figure 11.: Three-dimensional 3D plot for percentage Entrapment Efficiency (Y3)

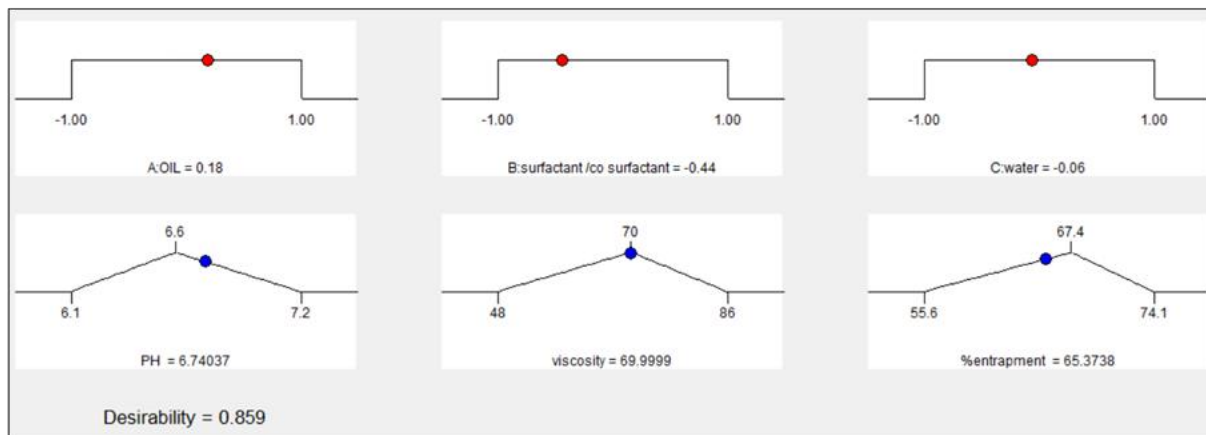


Figure 12.: Numerical optimization solution tool ramps for O1 formulation

Table 14.: Predicted and Observed values of dependent variables for Optimized formulation, O1

S. No.	Evaluation Parameter	Predicted Value	Observed Value
1.	pH	6.7	6.7 ± 0.2
2.	Viscosity	70	65.0 ± 3.0
3.	Percentage Entrapment efficiency	65.4	65.3 ± 0.3

* Observed vales have been expressed as Mean ± SD, n = 3

5.2. Particle Size Analysis

Dynamic Light Scattering (DLS) analysis revealed that the Z-average particle size of the formulation was 281.9 nm with a polydispersity index (PDI) of 0.274. These values confirm a moderately uniform nanoparticle distribution and fall within the ideal size range (<500 nm) for intranasal delivery, facilitating efficient mucosal permeation and potential nose-to-brain transport.

Figure 13

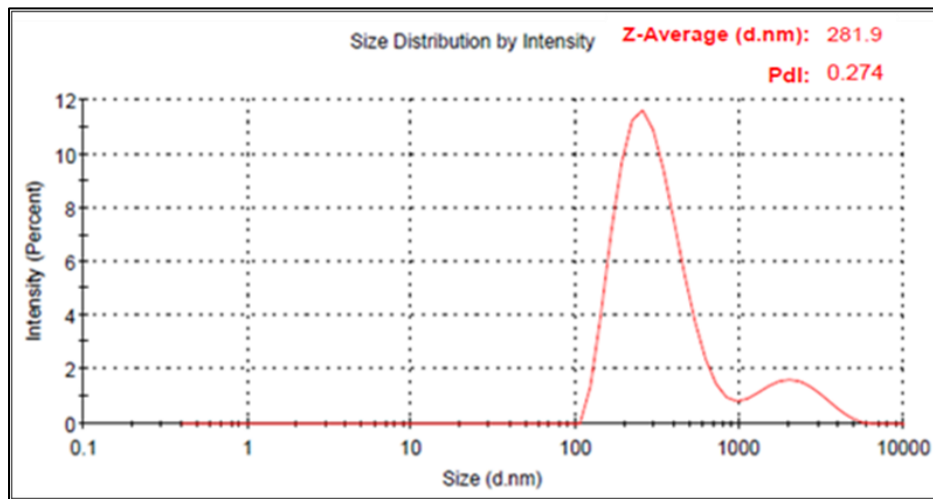


Figure 13.: Particle size analysis of optimized formulation, O1

5.3. Zeta Potential

Zeta Potential of the O1 formulation was measured at -4.96 mV, indicating a slightly negative surface charge. Although not highly charged, the value suggests sufficient electrostatic repulsion to maintain colloidal stability and prevent aggregation during storage. The sample exhibited 100% peak intensity, and a conductivity of 0.0277 mS/cm, with the result quality evaluated as "Good."

Figure 14

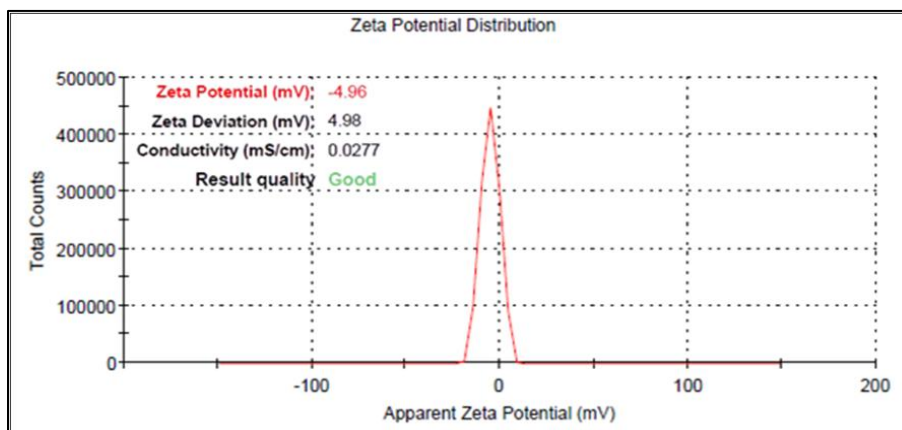


Figure 14.: Zeta Potential analysis of optimized formulation, O1

5.4. Scanning Electron Microscopy (SEM)

Scanning Electron Microscopy (SEM) analysis further confirmed that the nanoparticles were discrete, spherical, and uniformly distributed with minimal aggregation. The surface appeared smooth and non-porous, and no crystalline drug deposits were visible, indicating that Clonidine HCl was molecularly dispersed within the carrier matrix. Such morphology is favorable for enhancing mucosal adhesion and improving absorption efficiency. **Figure 15**

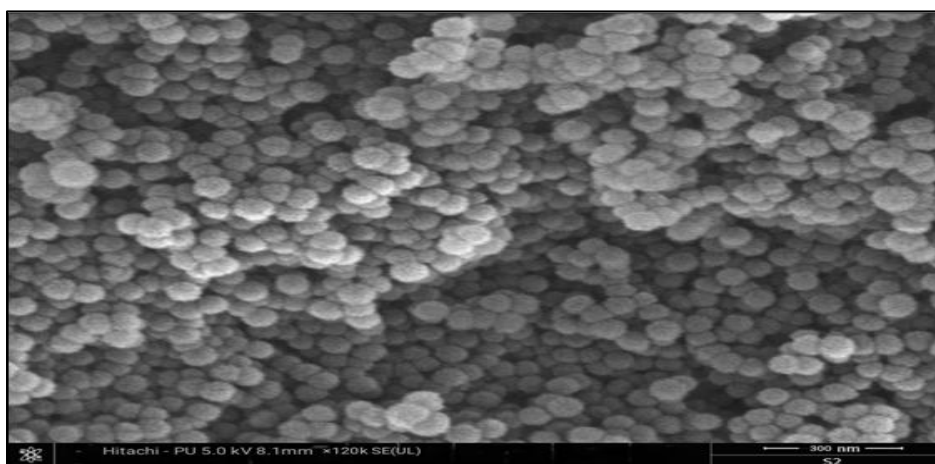


Figure 15.: SEM image of particles of optimized formulation, O1

5.5. Fourier-Transform Infrared Spectroscopy (FTIR)

Fourier-transform infrared spectroscopy (FTIR) was carried out to evaluate the compatibility of Clonidine HCl with excipients used in the microemulsion formulation and to confirm the chemical stability of the drug after formulation. The FTIR spectrum of the Clonidine HCl-loaded microemulsion (O1) shows the major characteristic absorption bands of Clonidine HCl along with peaks corresponding to formulation excipients. A broad and intense absorption band in the region of approximately $3200\text{--}3500\text{ cm}^{-1}$ is observed, which can be attributed to overlapping N–H stretching of Clonidine HCl and O–H stretching from surfactant/co-surfactant components, indicating possible physical hydrogen bonding interactions, which are common in microemulsion systems. The spectrum shows a distinct absorption band around $1600\text{--}1620\text{ cm}^{-1}$, corresponding to C=N stretching of the imidazoline ring of Clonidine HCl, confirming the retention of the drug's core structure. Additional bands in the region of $1500\text{--}1580\text{ cm}^{-1}$ are associated with aromatic C=C stretching vibrations, further supporting the integrity of the aromatic ring system. Characteristic aliphatic C–H stretching bands appear in the region of $2850\text{--}2950\text{ cm}^{-1}$, which are mainly attributed to the alkyl chains of Tween 80 and PEG 400 present in the formulation. A prominent absorption band observed near 1100 cm^{-1} corresponds to C–O–C stretching vibrations, indicative of ether linkages from PEG and surfactant molecules. The fingerprint region ($1500\text{--}600\text{ cm}^{-1}$) shows multiple bands corresponding to C–N stretching and aromatic C–H bending

vibrations, consistent with Clonidine HCl. Importantly, no disappearance of characteristic drug peaks or formation of new peaks was observed in the spectrum, suggesting that no chemical interaction or degradation of Clonidine HCl occurred during microemulsion formulation. This confirms good compatibility between Clonidine HCl and the selected excipients, with the drug remaining chemically stable within the microemulsion system. **Table 15, Figure 16**

Table 15: FTIR Range and Functional Groups Present in Clonidine HCl-Loaded Microemulsion Formulation (O1)

Functional Group / Bond	Typical Range (cm ⁻¹)	Observed (cm ⁻¹)	Interpretation
O–H / N–H stretching	3200–3500	Broad band ~3300–3500	Overlapping O–H and N–H stretching indicating hydrogen bonding and presence of drug and excipients
Aliphatic C–H stretching	2800–2950	~2850–2950	Due to alkyl chains of Tween 80 and PEG 400
C=N stretching (imidazoline ring)	1610–1640	~1600–1620	Confirms presence of Clonidine HCl
Aromatic C=C stretching	1500–1580	~1500–1580	Indicates intact aromatic ring structure
C–N stretching	1200–1300	~1250–1300	Associated with Clonidine HCl
C–O–C stretching (ether linkage)	1050–1150	~1080–1120	Attributed to PEG 400 and surfactant
Aromatic C–H bending	700–900	Present	Confirms aromatic nature of Clonidine HCl

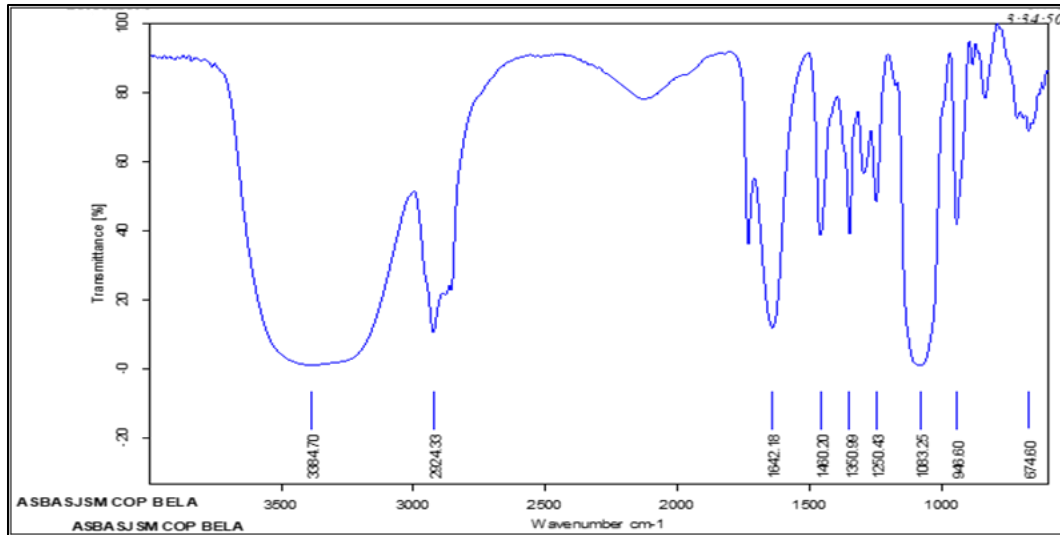


Figure 16.: Fourier transform infrared (FT-IR) of O1 formulation

5.6. Percentage Drug Content of optimized formulation, O1

Drug content analysis the drug content of the optimized formulation (O1) was determined to evaluate the drug entrapment efficiency and distribution neutrality in the nanoparticulate system. Drug content of the optimized formulation (O1) was 99.04% w/w, indicating high drug loading and negligible loss during processing of formulation. This large percentage indicate the compatibility of Clonidine Hydrochloride with the excipients used in selected formulation and to prove efficacy of method. The value is well within pharmacopeial acceptance limits for the drug content uniformity (usually, 85%–115%) that can be expected to give accurate and consistent dosing. Due to the precision, this is even more important in the case of INDSs that are designed for targeting the CNS, as high accuracy plays a prominent role in achieving therapeutic precision, consequently impacting pharmacological efficacy and patient safety. **Table 16**

Table 16: Percentage Drug content data of optimized formulation, O1

Formulation No.	Drug Content (% w/w) *
O1	99.04

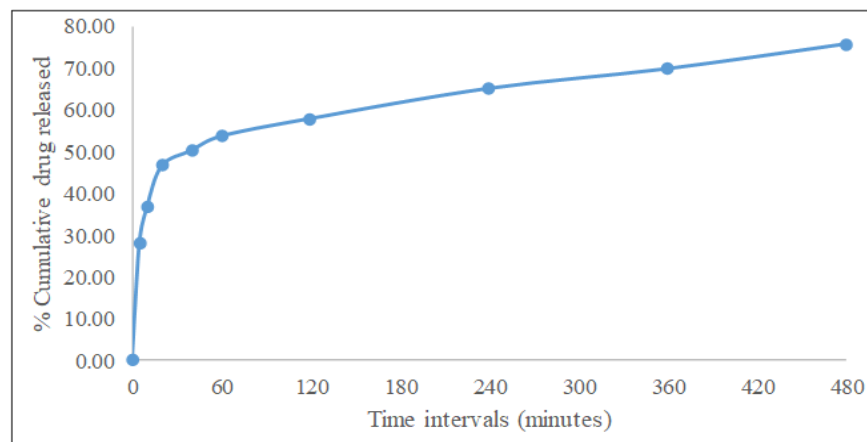
5.7. *In Vitro* Release Studies

In Vitro release studies of O1 exhibited a biphasic release profile. An initial burst release of $28.00 \pm 1.87\%$ was observed at 5 minutes, attributed to the drug adsorbed on or near the surface of the particles. This was followed by a controlled and sustained release, reaching $75.60 \pm 1.56\%$ over 480 minutes. Such a release profile is advantageous for maintaining prolonged therapeutic levels and reducing dosing frequency in anxiety treatment. **Table 17, Figure 17**

Table 17.: Percentage cumulative drug release vs Time intervals data of Optimized formulation, O1

time intervals (min)	% Cumulative drug released*
0	0.00 ± 1.17
5	28.00 ± 1.87
10	36.50 ± 0.96
20	46.50 ± 0.87
40	50.20 ± 1.56
60	53.60 ± 2.56
120	57.80 ± 3.54
240	65.00 ± 0.06
360	69.68 ± 0.58
480	75.60 ± 1.56

* Data has been expressed as Mean ± SD, n = 3

**Figure 17.: *In vitro* drug release profile of optimized formulation, O1**

5.8. Drug Release Kinetics of Optimized Formulation (O1)

Drug release kinetics were evaluated using zero-order, first-order, Higuchi, and Korsmeyer–Peppas models. The Korsmeyer–Peppas model demonstrated the best fit with an R^2 value of 0.9544, and an 'n' value of 0.1932, indicating Fickian diffusion as the dominant release

mechanism. The Higuchi model also showed a good correlation ($R^2 = 0.9077$), confirming diffusion-controlled drug release. Lower R^2 values for zero-order (0.7878) and first-order (0.7874) models indicated that the drug release was neither purely time- nor concentration-dependent.

Figure 18-21, Table 18

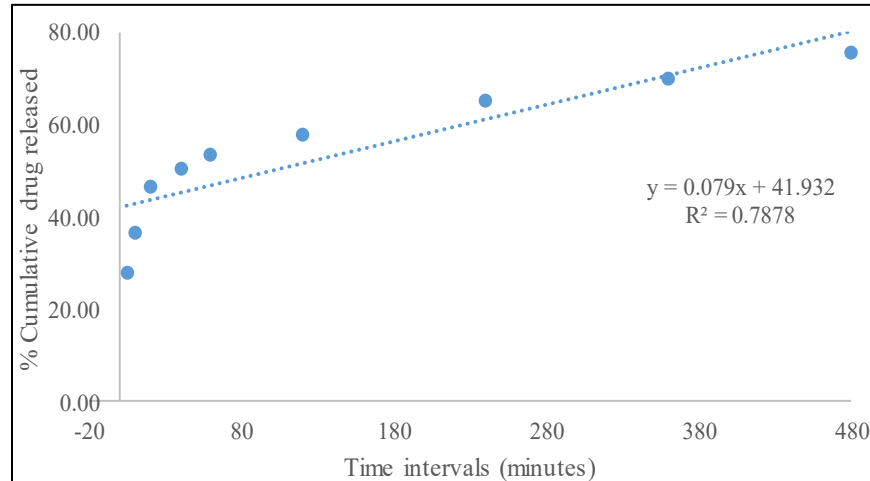


Figure 18.: Zero order release of optimized formulation, O1

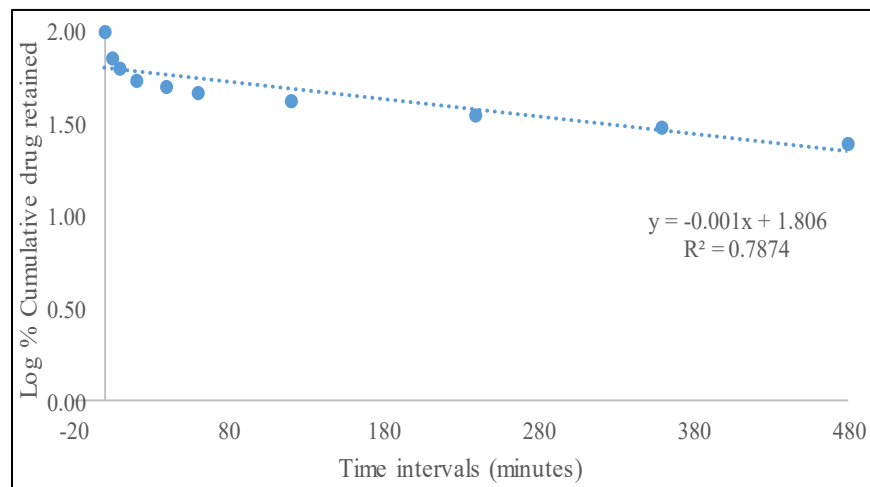


Figure 19.: First order graph of optimized formulation, O1

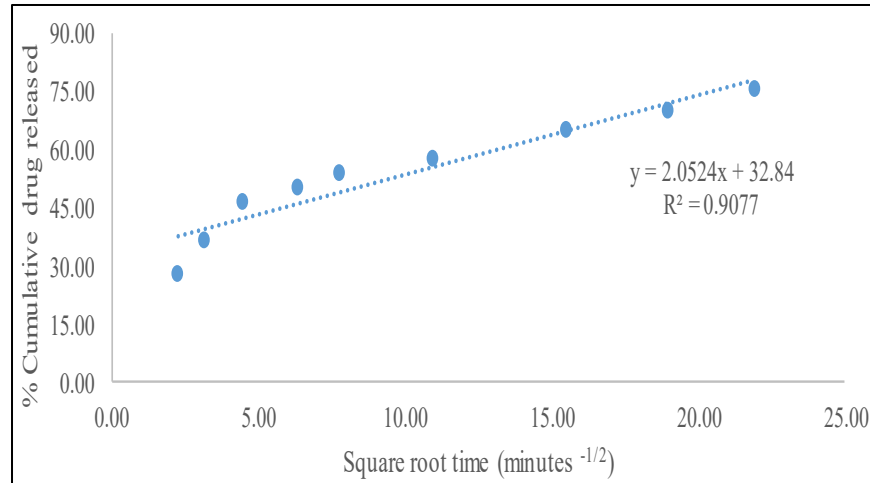


Figure 20.: Higuchi model graph of optimized formulation, O1

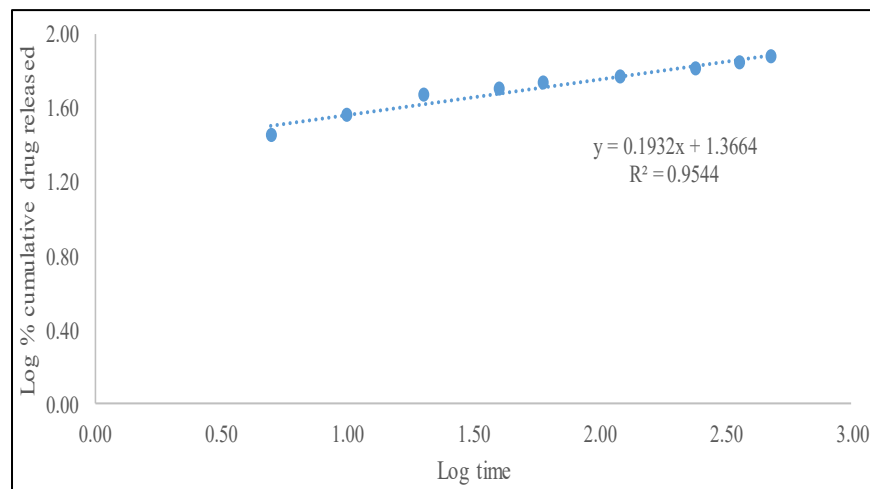


Figure 21.: Korsmeyer Peppas model of optimized formulation, O1

Table 18.: *In vitro* drug release kinetics studies data of Optimized formulation, O1

Model	Kinetics parameter	Observed values
Zero order Kinetics	k_0 (% sec ⁻¹)	0.079
	R^2	0.7878
First Order Kinetics	k_1 (sec ⁻¹)	-0.001
	R^2	0.7874
Higuchi Model	k_H (% cm ⁻² ·sec ^{-1/2})	2.0524
	R^2	0.9077

Korsmeyer-Peppas Model	K(sec⁻ⁿ)	0.1932
	R²	0.9544
	n	0.1932 (Fickian Diffusion)

5.9. Stability Studies

Accelerated stability testing of formulation O1 was conducted under ICH Q1A(R2)-specified conditions (40 ± 2 °C and $75 \pm 5\%$ RH) for a period of 30 days (1 month). The formulation was periodically evaluated for critical quality attributes including pH, viscosity, entrapment efficiency, and in vitro drug release. Across all intervals (0, 7-, 14-, 21-, and 30-days' time period), minimal variation was observed, indicating robust physicochemical stability. Furthermore, the similarity factor ($f_2 = 91.68$) between the initial and 30-day release profiles confirmed batch-to-batch consistency and long-term formulation reliability [66]. **Table 19, Figure 22**

Table 19.: Stability data of Optimized Formulation, O1

Accelerated conditions (40 °C \pm 2 °C / 75 %RH \pm 5 %RH)					
Parameter	0 day	7 days	14 days	21 days	30 days
Physical appearance	Stable	Stable	Stable	Stable	Stable
Color	Transparent	Transparent	Transparent	Transparent	Transparent
Odor	Odorless	Odorless	Odorless	Odorless	Odorless
pH	6.7 ± 0.2	6.6 ± 0.2	6.7 ± 0.5	6.7 ± 0.2	6.7 ± 0.8
Viscosity	65.0 ± 3.0	65.1 ± 1.0	65.1 ± 2.6	65.2 ± 3.0	65.0 ± 1.0
% EE	65.3 ± 0.3	65.2 ± 0.6	65.3 ± 0.4	65.2 ± 0.3	65.3 ± 0.5
% Drug Content	99.04 ± 0.5	98.87 ± 0.3	97.96 ± 0.8	97.54 ± 0.4	97.21 ± 0.6

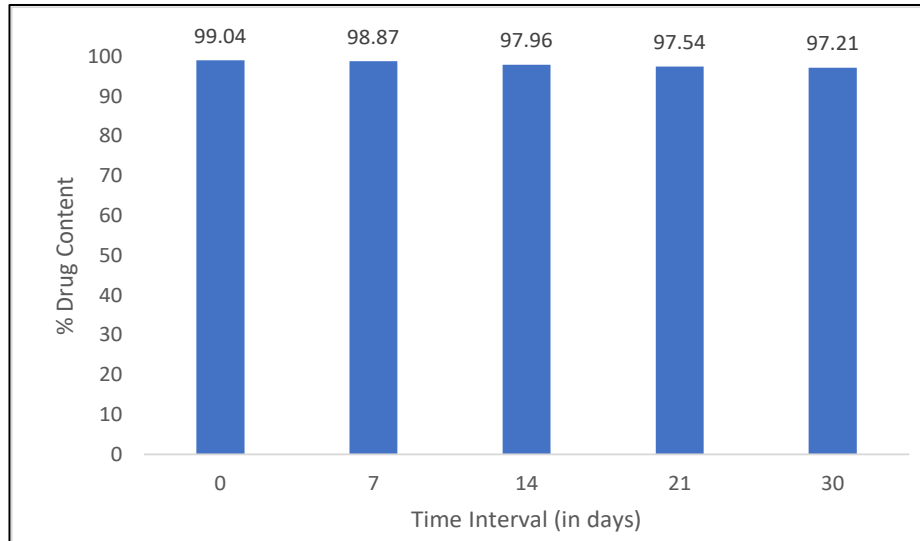


Figure 22.: % Drug Content comparison of optimized formulation at $t = 0$ days and 30 days evaluated under accelerated stability conditions ($40\text{ }^{\circ}\text{C} \pm 2\text{ }^{\circ}\text{C} / 75\% \text{RH} \pm 5\%$)

Dissolution Profile Comparison Under Stability Conditions

To evaluate the consistency of drug release behavior over time, a comparative in vitro dissolution study of the optimized formulation (O1) was conducted at initial (0-day) and post-accelerated storage (30-day) time points under ICH-recommended conditions ($40 \pm 2\text{ }^{\circ}\text{C} / 75 \pm 5\% \text{RH}$). The dissolution data were analyzed using model-independent statistical parameters—difference factor (f_1) and similarity factor (f_2)—to assess the level of similarity between the two profiles. The calculated f_1 value of 1.75 (well below the threshold of 15) and f_2 value of 91.68 (within the acceptable range of 50–100) indicated a high degree of similarity and minimal variation between the two dissolution curves. These results confirm that the formulation retained its release characteristics over the 30-day period, demonstrating robust physicochemical stability and supporting its suitability for long-term storage and clinical use in intranasal drug delivery. **Table 20, Figure 23**

Table 20.: *In vitro* drug release data of Optimized Formulation, O1 at Accelerated conditions (40 °C ± 2 °C / 75 %RH ± 5 %RH)

% Cumulative drug released		
time intervals (min)	0 days	30 days
0	00.00 ± 1.17	00.00 ± 1.17
5	28.00 ± 1.87	27.60 ± 1.07
10	36.50 ± 0.96	35.40 ± 0.88
20	46.50 ± 0.87	45.30 ± 0.78
40	50.20 ± 1.56	49.20 ± 1.06
60	53.60 ± 2.56	51.58 ± 2.45
120	57.80 ± 3.54	56.58 ± 0.54
240	65.00 ± 0.06	64.98 ± 0.26
360	69.68 ± 0.58	68.22 ± 0.65
480	75.60 ± 1.56	75.55 ± 1.28

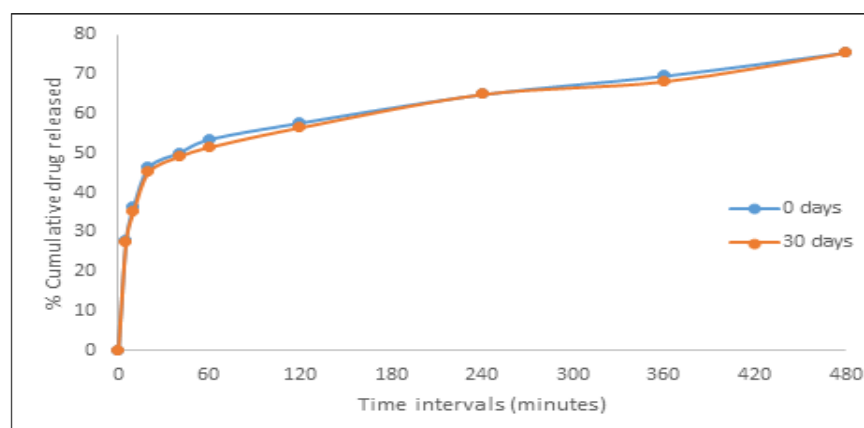


Figure 23.: Dissolution profile comparison of optimized formulation at t = 0 days and 30days evaluated under accelerated stability conditions (40 °C ± 2 °C / 75% RH ± 5%)

Stability Evaluation and Shelf-Life Estimation (T₉₀) of Optimized Clonidine Hydrochloride-Loaded Microemulsion

The stability of the optimized Clonidine Hydrochloride-loaded microemulsion formulation was

rigorously assessed under accelerated conditions ($40\text{ }^{\circ}\text{C} \pm 2\text{ }^{\circ}\text{C}$ / $75\% \text{ RH} \pm 5\%$) in accordance with ICH guidelines over a 30-day period. The formulation was periodically evaluated at intervals (0, 7, 14, 21, and 30 days) to monitor changes in drug content and in vitro release behavior. The drug content showed a slight decrease from 99.04% to 97.21%, indicating minimal degradation. To estimate the shelf life, the degradation kinetics were analyzed using a first-order kinetic model, expressed by the equation:

$$\log C = \log C_0 - (kt / 2.303), \dots \dots \dots \text{Equation(1)}$$

where C is the drug content at a given time t , C_0 is the initial content, and k is the degradation rate constant. Based on this model, the degradation rate constant (k) was calculated as 0.00068 day^{-1} , and the corresponding time for 10% degradation (t_{90}) was derived using the formula $t_{90} = 0.1052 / k$, yielding $t_{90} \approx 154$ days. Furthermore, dissolution profile comparison of day 0 and day 30 was performed using model-independent statistical methods. The difference factor (f_1) was found to be 1.75, and the similarity factor (f_2) was 91.68, both within acceptable regulatory limits, confirming no significant variation in drug release behavior during storage. Collectively, these findings indicate that the optimized microemulsion formulation of Clonidine Hydrochloride exhibits excellent physical and chemical stability, with consistent release performance, making it a promising candidate for long-term intranasal administration.

6. DISCUSSION

The current investigation focused on the development and optimization of an intranasal microemulsion-based nanoparticulate formulation of Clonidine Hydrochloride (Formulation O1) for the effective management of anxiety disorders. Employing a Central Composite Design (CCD) within a Quality by Design (QbD) framework allowed for a systematic exploration of formulation variables—namely the concentrations of isopropyl myristate (oil phase), surfactant/co-surfactant blend (Tween 80: PEG 400), and aqueous phase—and their influence on critical formulation attributes such as pH, viscosity, and entrapment efficiency.

The optimized formulation (O1) exhibited desirable physicochemical characteristics, including a pH of 6.7 ± 0.2 , confirming compatibility with the nasal mucosa, and a viscosity of $65.0 \pm 3.0 \text{ cPs}$, ideal for mucociliary retention and ease of administration. Entrapment efficiency was found to be $65.3 \pm 0.3\%$, indicating satisfactory drug encapsulation within the microemulsion matrix.

Dynamic light scattering (DLS) analysis revealed a mean particle size of 281.9 nm and a polydispersity index (PDI) of 0.274, suggesting a moderately uniform and monodisperse nanoparticulate system, suitable for enhanced absorption via olfactory and trigeminal nerve pathways. The formulation also exhibited a zeta potential of -4.96 mV , providing sufficient electrostatic repulsion to maintain colloidal stability over time. These findings are crucial, as particle size and surface charge greatly influence nasal deposition, mucosal permeability, and subsequent central nervous system (CNS) drug targeting.

Fourier-transform infrared (FTIR) spectroscopy confirmed the absence of significant chemical interactions between Clonidine HCl and formulation excipients, supporting the structural integrity and chemical stability of the formulation. The preservation of key functional group peaks in the spectrum validated compatibility. Scanning Electron Microscopy (SEM) further confirmed the formation of spherical, smooth-surfaced, and uniformly dispersed nanoparticles, which are favorable for mucosal adherence and consistent release behavior.

The drug content analysis of the optimized Clonidine Hydrochloride-loaded microemulsion formulation (O1) was conducted to evaluate the uniformity and efficiency of drug entrapment. The results demonstrated a drug content of $99.02 \pm 0.57\%$, indicating excellent drug incorporation within the microemulsion system. The high percentage reflects the precision of the formulation strategy and the compatibility of Clonidine Hydrochloride with the selected excipients. This also suggests minimal drug loss during the preparation process, ensuring reproducibility and stability of the formulation for potential therapeutic applications.

In vitro drug release studies demonstrated a biphasic release pattern with an initial burst release of $28.00 \pm 1.87\%$ within the first 5 minutes, followed by sustained drug release reaching $75.60 \pm 1.56\%$ at 480 minutes. This dual-phase profile is therapeutically beneficial for anxiety treatment, ensuring both rapid onset and extended symptom control. Kinetic modeling of the release data indicated that the formulation followed the Korsmeyer–Peppas model ($R^2 = 0.9544$), with an 'n' value of 0.1932, indicative of Fickian diffusion as the primary mechanism of drug release.

Stability studies performed under accelerated conditions ($40 \pm 2^\circ\text{C}$ and $75 \pm 5\%$ RH) for 28 days confirmed the robustness of the optimized formulation. No significant alterations were observed in pH, viscosity, entrapment efficiency, or release profile. The similarity factor ($f_2 = 91.68$) and difference factor ($f_1 = 1.75$) indicated a high degree of consistency between the initial and 28-day release profiles, thereby supporting the formulation's long-term stability and suitability for scale-up.

O1 was subjected to accelerated stability studies as per ICH guidelines ($40 \pm 2^\circ\text{C}$, $75 \pm 5\%$ RH) for 30 days. Various parameters such as organoleptic properties, pH, viscosity, entrapment efficiency, and drug release of the formulations were evaluated at 0, 7, 14, 21, and 30 days. The formulation remained clear and homogeneous during the experimentation period. pH was met with in the range of 6.6 ± 0.2 - 6.7 ± 0.8 , viscosity was approximately 65.0 cPs, and entrapment efficiency was quite constant at $65.3\% \pm$ little change.

The release profiles of the drugs throughout 30 days were also compared by model independent methods (difference factor f_1 and similarity factor f_2). The value of f_1 and f_2 were found to be 1.75 and 91.68, indicating high similarity between the release profiles of the batches. These findings confirm the physical stability of the formulation and its chemical stability during the storage period, indicating the stability and suitability of the developed formulation for the intended clinical use.

7. CONCLUSION

The study successfully demonstrates the formulation and optimization of a Clonidine Hydrochloride-loaded microemulsion-based nanoparticulate delivery system tailored for intranasal administration. The integration of a Central Composite Design under the QbD paradigm enabled robust optimization, ensuring reproducibility and enhanced product quality.

The optimized formulation (O1) exhibited ideal physicochemical properties, including mucosal-compatible pH, appropriate viscosity for nasal retention, nanosized particles for enhanced CNS penetration, and a high degree of drug & also good amount of Drug content. FTIR and SEM analyses confirmed chemical compatibility and structural integrity, while *in vitro* studies demonstrated a controlled and sustained drug release profile primarily governed by Fickian diffusion.

The intranasal route, leveraging direct nose-to-brain delivery via olfactory and trigeminal pathways, effectively bypasses the blood-brain barrier (BBB), thereby enhancing CNS bioavailability while minimizing systemic side effects. The observed pharmaceutical stability and Shelf-Life Estimation (T_{90}) under ICH-recommended conditions further substantiates the formulation's viability for extended storage and clinical translation.

In conclusion, the Clonidine HCl-loaded microemulsion presents a promising therapeutic strategy for anxiety management, combining non-invasive administration, enhanced brain targeting, and sustained release behavior. Future *in vivo* pharmacokinetic and pharmacodynamic evaluations are warranted to validate its clinical efficacy and potential for commercial development.

List of Abbreviations

How to cite this article: Singh et al. (2026). **Formulation and CCD-Based Optimization of Clonidine HCl-Loaded Microemulsion Nanoparticles for Intranasal Delivery in Anxiety Disorders.** *Pan-African Journal of Health and Psychological Sciences*. Vol 2, Issue 2, April-June 2026. <https://doi.org/10.64261/6x43w534>.

Abbreviation	Full Form
API	Active Pharmaceutical Ingredient
BBB	Blood-Brain Barrier
CCD	Central Composite Design
CNS	Central Nervous System
DLS	Dynamic Light Scattering
DSC	Differential Scanning Calorimetry
EE	Entrapment Efficiency
FTIR	Fourier Transform Infrared Spectroscopy
HCl	Hydrochloride
ICH	International Council for Harmonization
IPM	Isopropyl Myristate
MOF	Metal-Organic Framework
PEG 400	Polyethylene Glycol 400
PDI	Polydispersity Index
QbD	Quality by Design
RH	Relative Humidity
RSM	Response Surface Methodology
SEM	Scanning Electron Microscopy
Smix	Surfactant-Co-surfactant Mixture
UV	Ultraviolet Spectroscopy

***Conflicts of Interest:** *“The authors declare no conflicts of interest.”*

*** Funding Statement:** *“This research received no external funding.”*

References

1. Ashipala DO, Shilunga A. Overview and management of anxiety. In: Acceleration of the biopsychosocial model in public health. 2022. p. 194–210. doi:10.4018/978-1-6684-6496-0.ch009
2. Spielberger CD. Anxiety. In: Social problems in mental health. 2022. p. 15–19. doi:10.4324/9781003261919-7
3. Huneke N, Impey B, Baldwin D. Anxiety disorders. In: Cambridge textbook of neuroscience for psychiatrists. 2023. p. 410–415. doi:10.1017/9781911623137.059
4. Patil K, Reddy SK, RH D, L S, SK M. Evaluation of anxiolytic activity of encapsulated flaxseed oil alone and as an adjuvant in Swiss albino mice. *Int J Basic Clin Pharmacol*. 2017;6:2900. doi:10.18203/2319-2003.ijbcp20175215
5. Schnittker JS. Anxiety. In: Emotion in culture and everyday life. 2022. p. 133–149. doi:10.4324/9781003208556-9
6. Javaid SF, Hashim IJ, Hashim MJ, Stip E, Samad MA, Al Ahbabi A. Epidemiology of anxiety disorders: global burden and sociodemographic associations. *Middle East Curr Psychiatry*. 2023;30:44. doi:10.1186/s43045-023-00315-3
7. O’Leary KB, Khan JS. Pharmacotherapy for anxiety disorders. *Psychiatr Clin North Am*. 2024. doi:10.1016/j.psc.2024.04.012
8. Hoffman EJ, Mathew SJ. Anxiety disorders: a comprehensive review of pharmacotherapies. *Mt Sinai J Med*. 2008;75:248–262. doi:10.1002/msj.20041
9. Garakani A, Murrough JW, Freire RC, Thom RP, Larkin K, Buono FD, et al. Pharmacotherapy of anxiety disorders: current and emerging treatment options. *Front Psychiatry*. 2020;11:595584. doi:10.3389/fpsy.2020.595584
10. Outhoff K. An update on the pharmacological treatment of anxiety and related disorders. *S Afr Fam Pract*. 2016;58:50–56. doi:10.4102/safp.v58i5.4561
11. Sharma N, Kurmi BD, Singh D, Mehan S, Khanna K, Karwasra R, et al. Nanoparticles toxicity: mechanisms and mitigation strategies. *J Drug Target*. 2024;32:457–469. doi:10.1080/1061186x.2024.2316785
12. Sharma K. Recent advancement in drug delivery system for brain: an overview. *World J Pharm Pharm Sci*. 2017;7:292–305

13. Hersh DS, Wadajkar AS, Roberts N, Perez JG, Connolly NP, Frenkel V, et al. Evolving drug delivery strategies to overcome the blood–brain barrier. *Curr Pharm Des.* 2016;22:1177–1193. doi:10.2174/1381612822666151221150733
14. Wu D, Chen Q, Chen X, Han F, Chen Z, Wang Y. The blood–brain barrier: structure, regulation, and drug delivery. *Signal Transduct Target Ther.* 2023;8. doi:10.1038/s41392-023-01481-w
15. Abbott NJ, Patabendige AAK, Dolman DEM, Yusof SR, Begley DJ. Structure and function of the blood–brain barrier. *Neurobiol Dis.* 2010;37:13–25. doi:10.1016/j.nbd.2009.07.030
16. Pesavento M, Antunes J, Santos CA, Veiga F, Pires PC, et al. Brain targeting of antidepressant and anxiolytic drugs. 2022;31:50. doi:10.3390/asec2022-13766
17. Simhadri A, Dommeti MD, Sana J. Nanotechnology-based intranasal drug delivery systems for brain targeting. *J Pharma Insights Res.* 2024;2:15–23. doi:10.69613/fjsep132
18. Alotaibi TM, Alshehri OM, Alharby AMH, Alanazi KA, Alanazi AS, Alshahrany KDM, et al. Brain drug delivery: mechanisms and recent technologies. *Egypt J Chem.* 2024. doi:10.21608/ejchem.2024.332969.10716
19. Suzuki T, Suzuki N, Kanazawa T. Transport mechanism in nose-to-brain drug delivery and role of nanosystems. *Oleoscience.* 2020;20:61–69. doi:10.5650/oleoscience.20.61
20. Agosti E, Zeppieri M, Antonietti S, Battaglia L, Ius T, Gagliano C, et al. Lipid-based nanocarriers for CNS disorders: a systematic review. *Pharmaceutics.* 2024;16. doi:10.3390/pharmaceutics16030329
21. Koo J, Lim C, Oh KT. Intranasal administration for brain-targeting delivery: recent advances. *Int J Nanomedicine.* 2024;19:1767–1807. doi:10.2147/ijn.s439181
22. Liu Q, Zhang Q. Nanoparticle systems for nose-to-brain delivery. In: *Brain-targeted drug delivery systems.* 2019. p. 219–239. doi:10.1016/b978-0-12-814001-7.00010-x
23. Ren L, Fan Y, Wu W, Qian Y, He M, Li X, et al. Anxiety disorders: treatments, models, and circuitry mechanisms. *Eur J Pharmacol.* 2024;983:176994. doi:10.1016/j.ejphar.2024.176994
24. Sanghvi PG, Devi S. Synthesis of nanoparticles by microemulsion polymerization and their application in drug delivery. *Int J Polym Mater.* 2005;54:293–303. doi:10.1080/00914030390257359
25. Arredondo-Ochoa T, Silva-Martínez GA. Microemulsion-based nanostructures for drug delivery. *Front Nanotechnol.* 2022;3. doi:10.3389/fnano.2021.753947

26. Tan S, Stanslas J, Basri M, Karjiban RA, Kirby BP, Sani D, et al. Nanoemulsion-based parenteral delivery of carbamazepine. *Curr Drug Deliv.* 2015;12:795–804. doi:10.2174/1567201812666150901112544
27. Pires PC, Paiva-Santos AC, Veiga F. Nano and microemulsions for treatment of depressive and anxiety disorders. *Pharmaceutics.* 2022;14. doi:10.3390/pharmaceutics14122825
28. Grabrucker AM, Chhabra R, Belletti D, Forni F, Vandelli MA, Ruozi B, et al. Nanoparticles as blood–brain barrier permeable CNS drug delivery systems. *Top Med Chem.* 2014;10:71–90. doi:10.1007/7355_2013_22
29. Gold MS, Blum K. Clonidine. In: *Oxford handbook of opioids.* 2023. p. 543–570. doi:10.1093/oxfordhb/9780197618431.013.20
30. Dabbagh A. Clonidine: an old friend newly rediscovered. *Anesthesiol Pain Med.* 2011;1:8–9. doi:10.5812/kowsar.22287523.1802
31. Eldufani JB, Elahmer NR, Nekoui A, Blaise GA. Clonidine and dexmedetomidine: alpha-2 agonists in neuroscience. *Int J Basic Clin Pharmacol.* 2018;7:2476. doi:10.18203/2319-2003.ijbcp20184870
32. Shah NK, Al-Jindi P. Alpha-2 agonists. In: *Advances in anesthesia.* 2023. doi:10.1093/med/9780197584521.003.0046
33. Chodankar RS, Dev A. Optimisation techniques: a futuristic approach for formulating and processing of pharmaceuticals. *Indian J Pharm Biol Res.* 2016;4:32–40. doi:10.30750/ijphr.4.2.5
34. Abalos A, Maximo F, Manresa MA, Bastida J. Utilization of response surface methodology to optimize culture media for rhamnolipid production. *J Chem Technol Biotechnol.* 2002;77:777–784. doi:10.1002/jctb.637
35. Quinn GP, Keough MJ. *Experimental design and data analysis for biologists.* Cambridge: Cambridge University Press; 2002.
36. Myers RH, Montgomery DC, Anderson-Cook CM. *Response surface methodology: process and product optimization using designed experiments.* 4th ed. New York: Wiley; 2016.
37. Hassan M, Essam T, Yassin AS, Salama A. Optimization of rhamnolipid production using Plackett–Burman design. *Int J Biol Macromol.* 2016;82:573–579. doi:10.1016/j.ijbiomac.2015.09.057
38. Zhang M, Wang YY, Bai TC. Phase diagrams and viscosity of pseudoternary systems. *J Chem Eng Data.* 2012;57:2023–2029. doi:10.1021/je3003282

39. Berkman MS, Güleç K. Pseudo-ternary phase diagrams for microemulsion systems. *Istanbul J Pharm.* 2021;51:42–49. doi:10.26650/istanbuljpharm.2020.0090
40. Boonme P, Krauel K, Graf A, Rades T, Junyaprasert VB. Microemulsion characterization in pseudoternary systems. *AAPS PharmSciTech.* 2006;7:E99–E104. doi:10.1208/pt070245
41. Syed HK. Identification of phases of oil, surfactant/co-surfactant and water systems by ternary phase diagram. 2014.
42. Banker GS, Rhodes CT. *Modern pharmaceuticals.* 4th ed. New York: Marcel Dekker; 2002.
43. Bolton S, Bon C. *Pharmaceutical statistics: practical and clinical applications.* 5th ed. New York: Marcel Dekker; 2004.
44. Zhang C, Zhu Y, Zhang R, Xie Y, Wang K, Liu X. Pickering emulsions stabilized by modified nanoparticles. *RSC Adv.* 2015;5:90651–90658. doi:10.1039/c5ra10737g
45. Cui J, Sun S, Chen Z, Fan J, Hu J, Hu S, et al. Dual-responsive Pickering emulsions. *Colloids Surf A Physicochem Eng Asp.* 2023;679. doi:10.1016/j.colsurfa.2023.132550
46. Zhang W, Sun X, Fan X, Li M, He G. Alginate nanoparticle-stabilized Pickering emulsions. *J Dispers Sci Technol.* 2018;39:367–374. doi:10.1080/01932691.2017.1320223
47. Abdul-Razzaq R, Jaafar MZ, Bandyopadhyay S. Surfactant–nanoparticle synergy in emulsions. *J Phys Conf Ser.* 2020;1529:052059. doi:10.1088/1742-6596/1529/5/052059
48. Merchant RR, Maldonado-Camargo L, Rinaldi C. Viscosity of nanoparticle emulsions. *J Colloid Interface Sci.* 2017;486:241–248. doi:10.1016/j.jcis.2016.09.063
49. Bains U, Pal R. Continuous viscosity monitoring of emulsions. *Appl Sci.* 2019;9:4044. doi:10.3390/app9194044
50. Aboud HM, El Komy MH, Ali AA, El Menshawe SF, Abd Elbary A. Carvedilol solid lipid nanoparticles for intranasal delivery. *AAPS PharmSciTech.* 2016;17:1353–1365. doi:10.1208/s12249-015-0440-8
51. Joshi AS, Patel HS, Belgamwar VS, Agrawal A, Tekade AR. Ondansetron SLN for intranasal delivery. *J Mater Sci Mater Med.* 2012;23:2163–2175. doi:10.1007/s10856-012-4702-7

52. Yadav RK, Shah K, Dewangan HK. Sumatriptan SLN intranasal delivery. *Drug Dev Ind Pharm.* 2022;48:21–28. doi:10.1080/03639045.2022.2090575
53. Grossi C, Guccione C, Isacchi B, Bergonzi MC, Luccarini I, Casamenti F, et al. BBB-permeable nanoparticles. *Planta Med.* 2016;83:382–391. doi:10.1055/s-0042-101945
54. Aboutaleb E, Atyabi F, Khoshayand MR, Vatanara AR, Ostad SN, Kobarfard F, et al. Vincristine SLN brain delivery. *J Biomed Mater Res A.* 2014;102:2125–2136. doi:10.1002/jbm.a.34890
55. Lockman PR, Koziara JM, Mumper RJ, Allen DD. Nanoparticle surface charge and BBB permeability. *J Drug Target.* 2004;12:635–641. doi:10.1080/10611860400015936
56. Bhargavi C, Raghuvver P. Piribedil SLN nasal gel formulation. *Int J Pharm Qual Assur.* 2024;15:199–209. doi:10.25258/ijpqa.15.1.31
57. Mehmood Y, Shahid H, Barkat K, Ibraheem M, Riaz H, Badshah SF, et al. Mesoporous nanoparticles for nasal delivery. *Front Cell Dev Biol.* 2023;10:1026477. doi:10.3389/fcell.2022.1026477
58. Kadakia E, Bottino D, Amiji M. Nanoemulsion CNS transport modeling. *Pharm Res.* 2019;36:75. doi:10.1007/s11095-019-2610-y
59. Arya RKK, Vijay J, Bisht D, Rashid M, Alfawaz Altamimi AS, Afzal O, et al. Carbamazepine SLN brain delivery. *Curr Drug Deliv.* 2022;20:587–600. doi:10.2174/1567201819666220519120837
60. Chhabra R, Ruozi B, Vilella A, Belletti D, Mangus K, Pfaender S, et al. CNS nanoparticle delivery systems. *CNS Neurol Disord Drug Targets.* 2015;14:1041–1053. doi:10.2174/1871527314666150821111455
61. Nagaraju R, Rajeswari U, Ravi G, Bose PSC, Saritha D. Intranasal microemulsions for brain targeting. *Res J Pharm Technol.* 2021;14:2062–2068. doi:10.52711/0974-360x.2021.00366
62. Bohrey S, Chourasiya V, Pandey A. Diazepam polymeric nanoparticles. *Nano Converg.* 2016;3:3. doi:10.1186/s40580-016-0061-2
63. Chourasiya V, Bohrey S, Pandey A. Hydrochlorothiazide PLGA nanoparticles. *Polym Sci Ser B.* 2015;57:645–653. doi:10.1134/s1560090415060020
64. International Conference on Harmonisation (ICH). Stability testing of new drug substances and products Q1A(R2). 2003.
65. Diaz DA, Colgan ST, Langer CS, Bandi N, Likar MD, Van Alstine L. Dissolution similarity requirements. *AAPS J.* 2016;18:792. doi:10.1208/s12248-015-9835-4
66. Hill SA, Khan KA. Stability testing protocols. *Int J Pharm.* 1981;8:73–80. doi:10.1016/0378-5173(81)90011-9